

Published in final edited form as:

J Phys Chem Ref Data. 2016 September ; 45(3): . doi:10.1063/1.4958984.

Reference Correlations of the Thermal Conductivity of Ethene and Propene

M. J. Assael¹, A. Koutian¹, M. L. Huber², and R. A. Perkins²

¹Laboratory of Thermophysical Properties and Environmental Processes, Chemical Engineering Department, Aristotle University, Thessaloniki 54636, Greece

²Applied Chemicals and Materials Division, National Institute of Standards and Technology, 325 Broadway, Boulder, CO 80305, USA

Abstract

New, wide-range reference equations for the thermal conductivity of ethene and propene as a function of temperature and density are presented. The equations are based in part upon a body of experimental data that has been critically assessed for internal consistency and for agreement with theory whenever possible. For ethene, we estimate the uncertainty (at the 95% confidence level) for the thermal conductivity from 110 K to 520 K at pressures up to 200 MPa to be 5% for the compressed liquid and supercritical phases. For the low-pressure gas phase (to 0.1 MPa) over the temperature range 270 K to 680 K, the estimated uncertainty is 4%. The correlation is valid from 110 K to 680 K and up to 200 MPa, but it behaves in a physically reasonable manner down to the triple point and may be used at pressures up to 300 MPa, although the uncertainty will be larger in regions where experimental data were unavailable. In the case of propene, data are much more limited. We estimate the uncertainty for the thermal conductivity of propene from 180 K to 625 K at pressures up to 50 MPa to be 5% for the gas, liquid, and supercritical phases. The correlation is valid from 180 K to 625 K and up to 50 MPa, but it behaves in a physically reasonable manner down to the triple point and may be used at pressures up to 100 MPa, although the uncertainty will be larger in regions where experimental data were unavailable. For both fluids, uncertainties in the critical region are much larger, since the thermal conductivity approaches infinity at the critical point and is very sensitive to small changes in density.

Keywords

critical phenomena; ethene; ethylene; propene; propylene; reference correlations; thermal conductivity; transport properties

1. Introduction

In a series of recent papers, new reference correlations for the thermal conductivity of normal and parahydrogen,¹ water,² SF₆,³ toluene,⁴ benzene,⁵ *n*-hexane,⁶ *n*-heptane,⁷

Correspondence to: M. J. Assael.

^a) Partial contribution of NIST, not subject to copyright in the U.S.

methanol,⁸ ethanol,⁹ and *ortho*-xylene, *meta*-xylene, *para*-xylene and ethylbenzene,¹⁰ covering a wide range of conditions of temperature and pressure, were reported. In this paper, the work is extended to the thermal conductivity of ethene (commonly known as ethylene) and propene (commonly known as propylene).

The goal of this work is to critically assess the available literature data, and provide wide-ranging correlations for the thermal conductivity of ethene and propene that are valid over gas, liquid, and supercritical states, and incorporate densities provided by the equation of state of Smukala *et al.*¹¹ for ethene, and the recent equation of state of Lemmon *et al.*¹² for propene. It was decided to treat the two compounds in one paper, since they are quite similar in their thermophysical properties, and are often found together.

It should be noted that in 1983, Holland *et al.*¹³ published a correlation for the thermal conductivity of ethene covering a temperature range 110 to 500 K and pressure to 50 MPa, with an uncertainty of 5% increasing to 10% in the dense liquid range. Since 1983, new measurements have been published; in particular the measurements of Millat *et al.*,¹⁴ performed in an absolute transient hot-wire instrument with an uncertainty of 0.3–2%. These measurements were of particular importance, as the authors investigated the problems associated with the application of the transient hot-wire technique in the low-pressure gas region. Furthermore, after 1988, the behavior of the thermal conductivity in the critical region has been able to be modeled much better because of advances in theory.^{15, 16} These two factors allow us to propose an improved reference correlation for the thermal conductivity of ethene in this paper. In addition, we are unaware of any wide-ranging correlations for the thermal conductivity of propene, so the present work addresses that problem.

2. Methodology

The thermal conductivity, λ , is expressed as the sum of three independent contributions, as

$$\lambda(\rho, T) = \lambda_o(T) + \Delta\lambda(\rho, T) + \Delta\lambda_c(\rho, T) \quad (1)$$

where ρ is the density, T is the temperature, and the first term, $\lambda_o(T) = \lambda(0, T)$, is the contribution to the thermal conductivity in the dilute-gas limit, where only two-body molecular interactions occur. The final term, $\Delta\lambda_c(\rho, T)$, the critical enhancement, arises from the long-range density fluctuations that occur in a fluid near its critical point, which contribute to divergence of the thermal conductivity at the critical point. Finally, the term $\Delta\lambda(\rho, T)$, the residual property, represents the contribution of all other effects to the thermal conductivity of the fluid at elevated densities.

The identification of these three separate contributions to the thermal conductivity and to transport properties in general is useful because it is possible, to some extent, to treat both $\lambda_o(T)$ and $\Delta\lambda_c(\rho, T)$ theoretically. In addition, it is possible to derive information about $\lambda_o(T)$ from experiment. In contrast, there is almost no theoretical guidance concerning the

residual contribution, $\Delta\lambda(\rho, T)$, so that its evaluation is based entirely on experimentally obtained data.

The analysis described above should be applied to the best available experimental data for the thermal conductivity. Thus, a prerequisite to the analysis is a critical assessment of the experimental data. For this purpose, two categories of experimental data are defined: primary data employed in the development of the correlation, and secondary data used simply for comparison purposes. According to the recommendation adopted by the Subcommittee on Transport Properties (now known as The International Association for Transport Properties) of the International Union of Pure and Applied Chemistry, the primary data are identified by a well-established set of criteria.¹⁷ These criteria have been successfully employed to establish standard reference values for the viscosity and thermal conductivity of fluids over wide ranges of conditions, with uncertainties in the range of 1%. However, in many cases, such a narrow definition unacceptably limits the range of the data representation. Consequently, within the primary data set, it is also necessary to include results that extend over a wide range of conditions, albeit with a poorer accuracy, provided they are consistent with other more accurate data or with theory. In all cases, the accuracy claimed for the final recommended data must reflect the estimated uncertainty in the primary information.

2.1. The dilute-gas limit

In order to be able to extrapolate the temperature range of the measurements, a theoretically-based scheme was preferred in order to correlate the dilute-gas limit thermal conductivity, $\lambda_o(T)$, over a wide temperature range. The traditional kinetic approach for thermal conductivity results in an expression involving three generalized cross sections.^{18, 19} However, it is possible to derive an equivalent kinetic theory expression for thermal conductivity by making use of the approach of Thijssse *et al.*²⁰ and Millat *et al.*,²¹ where one considers expansion in terms of total energy, rather than separating translational from internal energy as is done traditionally. In this case, the dilute-gas limit thermal conductivity, $\lambda_o(T)$ ($\text{mW m}^{-1} \text{K}^{-1}$), of a polyatomic gas can be shown to be inversely proportional to a single generalized cross section,¹⁸⁻²¹ $S(10E)$ (nm^2), as

$$\lambda_o(T) = 1000 \frac{5k_B^2(1+r^2)T}{2m\langle\nu\rangle_o S(10E)} f_\lambda, \quad (2)$$

where k_B is the Boltzmann constant, $T(\text{K})$ is the absolute temperature, f_λ is the dimensionless higher-order correction factor, m (kg) is the molecular mass, and

$\langle\nu\rangle_o = 4\sqrt{k_B T/\pi m}$ (m/s) is the average relative thermal speed. The quantity r^2 is defined by $r^2 = 2C_{\text{int}}^o/5k_B$, where C_{int}^o is the contribution of both the rotational, C_{rot}^o , and the vibrational, C_{vib}^o , degrees of freedom to the isochoric ideal-gas heat capacity C_v^o .

The recent classical trajectory calculations²²⁻²⁴ confirm that for most molecules studied, the higher-order thermal-conductivity correction factor is near unity. One can take advantage of

this finding to define the effective generalized cross section $S_\lambda (= S(10E)/f_\lambda)$ (nm^2), and rewrite Eq. (2) for the dilute-gas limit thermal conductivity, $\lambda_o(T)$ ($\text{mW m}^{-1} \text{K}^{-1}$), as

$$\lambda_o(T) = C_\lambda \frac{(C_p^o/k_B) \sqrt{T}}{S_\lambda}, \quad (3)$$

where C_λ is a constant obtained from the molecular mass and Eq. (2) for each fluid, and the ideal-gas isobaric heat capacity, $C_p^o (= C_{\text{int}}^o + 2.5 k_B)$ in (J/K), can be obtained from the literature.

It has been previously noted,²¹ and recently confirmed¹⁹ for smaller molecules, that the cross section $S(10E)$ exhibits a nearly linear dependence on the inverse temperature. Hence, experimental data will be employed to obtain coefficients a_0 (nm^2), and a_1 ($\text{nm}^2 \text{K}$), in

$$S_\lambda = a_0 + a_1/T. \quad (4)$$

Although the scheme described by Eqs. (3) and (4) is strictly valid for smaller molecules, it has been found to work very well as a correlation tool for larger molecules.^{4, 5, 7, 9} Hence, Eqs. (3) and (4) form a consistent set of equations for the calculation of the dilute-gas limit thermal conductivity.

2.2. The residual thermal conductivity

The thermal conductivities of pure fluids exhibit an enhancement over a large range of densities and temperatures around the critical point and become infinite at the critical point. This behavior can be described by models that produce a smooth crossover from the singular behavior of the thermal conductivity asymptotically close to the critical point to the residual values far away from the critical point.^{15, 25, 26} The density-dependent terms for thermal conductivity can be grouped according to Eq. (1) as $[\Delta\lambda(\rho, T) + \Delta\lambda_c(\rho, T)]$. To assess the critical enhancement theoretically, we need to evaluate, in addition to the dilute-gas thermal conductivity, the residual thermal-conductivity contribution. The procedure adopted during this analysis used ODRPACK (Ref. 27) to fit all the primary data simultaneously to the residual thermal conductivity and the critical enhancement, while maintaining the values of the dilute-gas thermal-conductivity data already obtained. The density values employed were obtained by the equation of state of Smukala *et al.*¹¹ for ethene and Lemmon *et al.*¹² for propene. The primary data were weighted in inverse proportion to the square of their uncertainty.

The residual thermal conductivity was represented with a polynomial in temperature and density:

$$\Delta\lambda(\rho, T) = \sum_{i=1}^5 (B_{1,i} + B_{2,i}(T/T_c)) (\rho/\rho_c)^i. \quad (5)$$

Coefficients $B_{1,i}$ and $B_{2,i}$ will be obtained for each fluid separately, employing the corresponding primary data.

2.3. The critical enhancement

The theoretically based crossover model proposed by Olchowy and Sengers^{15, 25, 26} is complex and requires solution of a quartic system of equations in terms of complex variables. A simplified crossover model has also been proposed by Olchowy and Sengers.¹⁶ The critical enhancement of the thermal conductivity from this simplified model is given by

$$\Delta\lambda_c = \frac{\rho C_p R_D k_B T}{6\pi\bar{\eta}\xi} (\bar{\Omega} - \bar{\Omega}_0), \quad (6)$$

with

$$\bar{\Omega} = \frac{2}{\pi} \left[\left(\frac{C_p - C_v}{C_p} \right) \arctan(\bar{q}_D \xi) + \frac{C_v}{C_p} \bar{q}_D \xi \right] \quad (7)$$

and

$$\bar{\Omega}_0 = \frac{2}{\pi} \left[1 - \exp \left(- \frac{1}{(\bar{q}_D \xi)^{-1} + (\bar{q}_D \xi \rho_c / \rho)^2 / 3} \right) \right]. \quad (8)$$

In Eqs. (6)–(8), k_B is Boltzmann's constant, $\bar{\eta}$ is the viscosity, and C_p and C_v are the isobaric and isochoric specific heat obtained from the literature for each fluid. The correlation length ξ is given by

$$\xi = \xi_0 \left(\frac{p_c \rho}{\Gamma \rho_c^2} \right)^{\nu/\gamma} \left[\left. \frac{\partial \rho(T, \rho)}{\partial p} \right|_T - \left(\frac{T_{\text{ref}}}{T} \right) \left. \frac{\partial \rho(T_{\text{ref}}, \rho)}{\partial p} \right|_T \right]^{\nu/\gamma}. \quad (9)$$

In the above equations for the two fluids studied, values for the universal amplitude, $R_D = 1.02$ (–), and the universal critical exponents, $\nu = 0.63$ and $\gamma = 1.239$ were employed, using a universal representation of the critical enhancement of the thermal conductivity (based on a simplified solution of mode-coupling theory with fluid-specific parameters determined by a corresponding states method) by Perkins *et al.*²⁸ Furthermore, for each fluid, the same

scheme was employed to estimate the values of $\Gamma(m)$ and $\xi_0(m)$, the amplitudes of the asymptotic power laws, while the effective cutoff wavelength $\bar{q}_D^{-1}(m)$ was calculated by employing the selected primary experimental data.

3. Thermal-Conductivity Correlations

3.1. The correlation for ethene

Table 1 summarizes, to the best of our knowledge, the experimental measurements of the thermal conductivity of ethene reported in the literature. From the 25 sets shown in the table, 16 were considered as primary data.

The measurements of Millat *et al.*¹⁴ are the most accurate data available, and were obtained in an absolute transient hot-wire instrument employing two Pt wires, with uncertainties of 0.3% rising to 2% near the critical point, based on a full theoretical model proven to operate with such an uncertainty. Measurements performed by this group (of W.A. Wakeham of Imperial College London) have already been successfully employed in many thermal conductivity reference correlations.^{4-7, 10} The measurements of Golubev *et al.*,³⁵ extending to a very wide range of temperatures and pressures, were performed in an absolute hot-wire instrument with an uncertainty of 1.5% rising to 3% near the critical region. Measurements from this investigator have also been successfully employed in previous reference correlations,^{6, 8, 9} and thus were also considered as primary data. A hot-wire instrument was also employed by Tarzimanov and Lozovoi³³ and Tarzimanov and Arshlanov³⁴ to perform measurements at higher temperatures and pressures, with an uncertainty of 1.5% rising to 3% near the critical region. Measurements of this group have also been successfully employed in previous reference correlations.^{8, 9} The measurements of Prasad and Venart³¹ performed in an absolute transient hot-wire instrument with an uncertainty of 1.5% also extended to higher pressures, and were thus included in the primary data. The measurements of Vargaftik and Vanicheva,³² performed in a hot-filament instrument with an uncertainty of 1-2%, were also included in the primary data set as they extend to higher temperatures. Measurements at higher temperatures were also performed by Senftleben^{36, 38} and Senftleben *et al.*⁴⁰ in a concentric-cylinder instrument with an uncertainty of 1-2%. Concentric-cylinder instruments were also employed by Zheng *et al.*,²⁹ Yorizane *et al.*,³⁰ and Lenoir and Comings³⁹ with uncertainties of 3, 3, and 1.5% respectively; thus these sets were also included in the primary data sets. The measurements of Lambert *et al.*,³⁷ performed in a hot-wire apparatus have been successfully employed in previous reference correlations.⁵⁻⁸ Finally the measurements of Borovick,⁴¹ Borovick *et al.*,⁴² and Eucken⁴³ were included in the primary data set, as they extend to low temperatures. The remaining sets were considered as secondary data.

Figures 1 and 2 show the range of the primary measurements outlined in Table 1, and the saturation curve may be seen in Fig. 2. Temperatures for all data were converted to the ITS-90 temperature scale.⁵³ The development of the correlation requires accurate values for the density; Smukala *et al.*¹¹ have reviewed the thermodynamic properties of ethene and developed an accurate, wide-ranging equation of state. For the density, the estimated uncertainty of the new equation of state is less than $\pm 0.02\%$ for pressures up to 12 MPa and

temperatures up to 340 K with the exception of the critical region. Outside the range mentioned above, the estimated uncertainty is less than $\pm 0.03\%$ for pressures up to 30 MPa and temperatures between 235 and 350 K. We also adopt their values for the critical temperature, T_c , the critical density, ρ_c , and the triple-point temperature as 282.35 K, 214.24 kg m⁻³, and 103.986 K, respectively. Finally, as already mentioned, the isobaric ideal-gas heat capacity was also obtained from the same source.¹¹

3.1.1. The dilute-gas limit of ethene—Substituting in Eq. (2) the molecular mass [(0.028 053 76/6.022 140 857×10²³) kg]¹¹ of ethene, Eq. (3), becomes

$$\lambda_o(T) = 0.1053223 \frac{(C_p^o/k_B) \sqrt{T}}{S_\lambda}, \quad (10)$$

The isobaric heat capacity, $C_p^o (=C_{\text{int}}^o + 2.5 k_B)$, can be obtained from Smukala *et al.*¹¹ as

$$\frac{C_p^o}{k_B} = 1 + a_0 + \sum_{i=1}^4 a_i (\theta_i \tau)^2 \frac{\exp(\theta_i \tau)}{[\exp(\theta_i \tau) - 1]^2}, \quad (11)$$

where $\tau = T_c/T$ is the inverse reduced temperature. The values of the coefficients a_i and θ_i are: $a_0 = 3.0$, $a_1 = 2.49395851$, $a_2 = 3.00271520$, $a_3 = 2.51265840$, $a_4 = 3.99064217$, $\theta_1 = 4.43266896$, $\theta_2 = 5.74840149$, $\theta_3 = 7.80278250$, $\theta_4 = 15.5851154$.

It is now known^{54, 55} that the transient hot-wire technique should not be applied to the low-pressure low-density gas region; this problem is still under investigation. Keeping this in mind, Millat *et al.*¹⁴ performed very accurate measurements of the thermal conductivity down to 0.4 MPa, and employed their measurements to extrapolate to zero density. These measurements were included in the primary data set. For exactly this reason, all other measurements performed in transient hot-wire or hot-wire instruments in the dilute-gas region were not included in the primary data set. The remaining investigators^{29, 30, 36, 38–40} in the primary-data section of Table 1, who performed measurements with different instruments (other than THW) in the low-pressure low-density gas region, were included as primary data in the correlation. These measurements were employed together with Eqs. (10) and (11) in order to obtain the coefficients a_0 (nm²), and a_1 (nm² K), of Eq. (4), as

$$S_\lambda = 0.129 + 96.085/T. \quad (12)$$

Equations (10)–(12) form a consistent set of equations for the calculation of the dilute-gas limit thermal conductivity of ethene.

The values of the dilute-gas limit thermal conductivity, $\lambda_0(T)$ in $\text{mW m}^{-1} \text{K}^{-1}$, obtained by the scheme of Eqs. (10)–(12), were fitted as a function of the reduced temperature $T_r = T/T_c$ for ease of use to the following equation:

$$\lambda_0(T) = \frac{-54.1761 + 541.904T_r - 656.108T_r^2 + 667.048T_r^3 - 109.992T_r^4 + 60.6511T_r^5 - 1.01377T_r^6}{26.5363 - 20.1401T_r + 19.4152T_r^2 - 2.92695T_r^3 + T_r^4} \quad (13)$$

Values calculated by Eq. (13) do not deviate from the values calculated by the scheme of Eqs. (10)–(12) by more than 0.02% over the temperature range from 180 K to 680 K. Equation (13) is hence employed in the calculations that will follow.

Figure 3 shows the primary dilute-gas thermal-conductivity values of the selected investigators, and the values calculated by Eqs. (10)–(12), as well as the values calculated by the previous correlation of Holland *et al.*,¹³ as a function of the temperature. In Fig. 4, percentage deviations of the primary dilute-gas thermal-conductivity values of ethene from the scheme of Eqs. (10)–(12) are also shown. They all agree with the present correlation within a maximum deviation of 4%. Based on these measurements, the uncertainty of the correlation, at the 95% confidence level over the temperature range 270 K to 680 K, is 4%. The correlation behaves in a physically reasonable manner over the entire range from the triple point to the highest temperature of the experimental data, 673 K; however, we anticipate the uncertainty may be larger in the areas where data are unavailable and the correlation is extrapolated.

In Fig. 5, the remaining dilute-gas thermal-conductivity values are shown. These consist of the transient hot-wire and hot-wire primary measurements at low pressures that, as mentioned earlier, are inaccurate in the dilute-gas region, and all the secondary dilute-gas thermal conductivity measurements. The distinct difference in slope is in large part attributed to this effect of employing the transient hot-wire technique in the dilute-gas region. We note that the correlation of Holland *et al.*¹³ was based only on this group of measurements, since the measurement of Millat *et al.*¹⁴ were obtained later.

3.1.2. The residual and the critical-enhancement contributions of ethene—As already mentioned, the coefficients $B_{1,j}$ and $B_{2,j}$ in Eq. (5) and the effective cutoff wavelength \bar{q}_D^{-1} were fitted with ODRPACK²⁷ to the primary data for the thermal conductivity of ethene. The value of $\bar{q}_D^{-1} = 4.9 \times 10^{-10} \text{ m}$ was found. The crossover model requires the system-dependent amplitudes Γ and ξ_0 . For this work, the system-dependent amplitudes Γ and ξ_0 were estimated as $\Gamma = 0.058$, $\xi_0 = 1.81 \times 10^{-10} \text{ m}$, using the universal representation of the critical enhancement of the thermal conductivity by Perkins *et al.*²⁸ The viscosity required for Eq. (6) was calculated with the correlation of Holland *et al.*¹³ The reference temperature T_{ref} , far above the critical temperature where the critical enhancement

is negligible, was calculated by $T_{\text{ref}} = (3/2) T_c$,⁵⁶ which for ethene is 423.53 K. The coefficients $B_{1,i}$ and $B_{2,i}$ of Eq. (5) obtained are shown in Table 2.

Table 3 summarizes comparisons of the primary data with the correlation. We have defined the percentage deviation as $\text{PCTDEV} = 100 * (\lambda_{\text{exp}} - \lambda_{\text{fit}}) / \lambda_{\text{fit}}$, where λ_{exp} is the experimental value of the thermal conductivity and λ_{fit} is the value calculated from the correlation. Thus, the average absolute percentage deviation (AAD) is found with the expression $\text{AAD} = (\sum |\text{PCTDEV}|) / n$, where the summation is over all n points, and the bias percent is found with the expression $\text{BIAS} = (\sum \text{PCTDEV}) / n$. We estimate the uncertainty (at the 95% confidence level) for the thermal conductivity in the liquid and supercritical phases from 110 K to 520 K and up to 200 MPa, to be 5%. Uncertainties in the critical region are much larger, since the thermal conductivity approaches infinity at the critical point and is very sensitive to small changes in density.

Figure 6 shows the percentage deviations of all primary thermal–conductivity data from the values calculated by Eqs. (1), (5)–(9), and (13), as a function of density. Figures 7 and 8 show the same deviations but as a function of temperature and pressure, respectively.

Table 4 shows the average absolute percentage deviation (AAD) and the bias for the secondary data. Finally, Figs. 9 and 10 show plots of the thermal conductivity of ethene as a function of the temperature for different pressures, and as a function of the density for different temperatures.

3.1.3. Empirical critical enhancement—For applications at state points that are relatively distant from the critical point (at least 10–15 K from the critical temperature), the critical enhancement is adequately represented by the following empirical expression:

$$\Delta\lambda_c(\rho, T) = \frac{C_1}{C_2 + |\Delta T_c|} \exp \left[-(C_3 \Delta\rho_c)^2 \right], \quad (14)$$

where $\Delta T_c = (T/T_c) - 1$ and $\Delta\rho_c = (\rho/\rho_c) - 1$. This equation does not require accurate information on the compressibility, specific heat, and viscosity of ethene in the critical region, as does the theory of Olchow and Sengers.^{15, 26, 28} The coefficients of Eqs. (8) and (9) were fixed, while the coefficients of Eq. (14) were fitted to the primary data. The values obtained were $C_1 = 0.20 \text{ mW m}^{-1} \text{ K}^{-1}$, $C_2 = 0.30$, and $C_3 = 0.09$.

3.1.4. Recommended Values—In Table 5, recommended values for the thermal conductivity are shown. For checking computer implementations of the correlation, a point is provided for testing code with critical enhancement at 300.0 K and 300.0 kg m^{-3} (8.8571 MPa), where the thermal conductivity is $69.62 \text{ mW m}^{-1} \text{ K}^{-1}$; the dilute–gas thermal conductivity, $\lambda_o(300 \text{ K}) = 21.01 \text{ mW m}^{-1} \text{ K}^{-1}$, the residual term $\Delta\lambda(300.0 \text{ kg m}^{-3}, 300 \text{ K}) = 44.48 \text{ mW m}^{-1} \text{ K}^{-1}$, and the critical enhancement term, $\Delta\lambda_c(300.0 \text{ kg m}^{-3}, 300 \text{ K}) = 4.12 \text{ mW m}^{-1} \text{ K}^{-1}$. The viscosity used in the calculation of the enhancement for this state point is $33.791 \text{ }\mu\text{Pa s}$, obtained from the correlation of Holland *et al.*¹³

3.2. The correlation for propene

Table 6 summarizes, to the best of our knowledge, the experimental measurements of the thermal conductivity of propene reported in the literature. Only 9 sets of measurements were found.

The measurements of Yata *et al.*⁵⁷ and Swift and Migliori⁵⁸ were both obtained in transient hot-wire instruments backed by a full theory, with an uncertainty of 1% and 3% respectively. These measurements were considered as primary data. The measurements of Parkinson *et al.*,⁵⁹ although a bit older than the previous ones, were also performed in a transient hot-wire instrument with a 2% uncertainty, and were part of the primary data set. Furthermore, for the reason given in Section 3.1.1 in propene, the measurements of Senftleben,^{36, 38} Senftleben *et al.*,⁴⁰ and Lambert *et al.*³⁷ also formed part of the primary dataset. However the last three temperatures (over 423 K) of Senftleben *et al.*⁴⁰ were disregarded because they showed unexpected large deviations from the rest of the data. Finally, two more sets of measurements were considered as primary data for propene, although they were not so, in the case of ethene: a) the measurements of Kolomiets⁴⁶ performed in a hot-wire instrument with unknown uncertainty, and b) the measurements of Naziev⁶⁰ performed in a concentric cylinder instrument with a 1.4% uncertainty. These two sets of measurements in the case of ethene showed larger deviations than the rest of the measurements, and since in ethene there existed a large number of additional data, these were regarded as secondary. However, in the case of propene, the lack of measurements forces us to consider these two sets as primary, but with a lower weight.

Figures 11 and 12 show the range of the primary measurements outlined in Table 6, and the saturation curve may be seen in Figure 12. Temperatures for all data were converted to the ITS–90 temperature scale.⁵³ The development of the correlation requires accurate values for the density; Lemmon *et al.*¹² have reviewed the thermodynamic properties of propene and developed an accurate, wide-ranging equation of state. For the density, the estimated uncertainty of the new equation of state is less than $\pm 0.02\%$ for pressures up to 30 MPa and temperatures up to 400 K with the exception of the critical region. We also adopt their values for the critical temperature, T_c , the critical density, ρ_c , and the triple-point temperature as 364.211 K, 229.63 kg m⁻³, and 87.953 K, respectively.¹² Finally, as already mentioned, the isobaric ideal-gas heat capacity was also obtained from the same source.

3.2.1. The dilute-gas limit of propene—Substituting in Eq. (2) the molecular mass [(0.042 080/6.022 140 857 $\times 10^{23}$) kg] of propene, Eq. (3) becomes

$$\lambda_o(T) = 0.0859960 \frac{(C_p^o/k_B) \sqrt{T}}{S_\lambda} \quad (15)$$

The isobaric heat capacity, $C_p^o (=C_{\text{int}}^o + 2.5 k_B)$, can be obtained from Lemmon *et al.*¹² as

$$\frac{C_p^o}{k_B} = 1 + \nu_0 + \sum_{k=1}^4 \nu_k (u_k/T)^2 \frac{\exp(u_k/T)}{[\exp(u_k/T) - 1]^2}, \quad (16)$$

where $\nu_0 = 3$, $\nu_1 = 1.544$, $\nu_2 = 4.013$, $\nu_3 = 8.923$, $\nu_4 = 6.02$, $u_1 = 324$ K, $u_2 = 973$ K, $u_3 = 1932$ K, $u_4 = 4317$ K.

The dilute-gas measurements^{36–38, 40, 46, 59, 60} of Table 6 were employed, together with Eqs. (15) and (16), in order to obtain the coefficients a_0 (nm²), and a_1 (nm² K), of Eq. (4), as

$$S_\lambda = 0.2998 + 108.12/T. \quad (17)$$

Equations (15)–(17) form a consistent set of equations for the calculation of the dilute-gas limit thermal conductivity of propene.

The values of the dilute-gas limit thermal conductivity, $\lambda_0(T)$ in mW m⁻¹ K⁻¹, obtained by the scheme of Eqs. (15)–(17), were fitted as a function of the reduced temperature $T_r = T/T_c$ for ease of use to the following equation:

$$\lambda_0(T) = \frac{-1.37218 + 17.3386T_r - 3.27682T_r^2 + 9.34452T_r^3 + 12.88T_r^4 - 1.5705T_r^5}{1.39367 - 1.04648T_r + T_r^2}. \quad (18)$$

Values calculated by Eq. (18) do not deviate from the values calculated by the scheme of Eqs. (15)–(17) by more than 0.04% over the temperature range from 150 K to 700 K. Equation (18) is hence employed in the calculations that will follow.

Figure 13 shows the primary dilute-gas thermal-conductivity values of the selected investigators, and the values calculated by Eq. (18). In Fig. 14, percentage deviations of the primary dilute-gas thermal-conductivity values of propene from the scheme of Eqs. (15)–(17) are also shown. Except for the three highest temperature values of Senftleben,³⁶ which show an inexplicable very high deviation from the rest of the measurements (and were consequently disregarded), the remaining data agree with the present correlation within a maximum deviation of 5%. Based on these measurements, the uncertainty of the correlation, at the 95% confidence level over the temperature range 180 K to 625 K, is 5%. The correlation behaves in a physically reasonable manner over the entire range from the triple point to 750 K; however, we anticipate the uncertainty may be larger in the areas where data are unavailable and the correlation is extrapolated.

3.2.2. The residual and the critical-enhancement contributions of propene—As already mentioned, the coefficients $B_{1,i}$ and $B_{2,i}$ in Eq. (5) and the effective cutoff wavelength \bar{q}_D^{-1} , were fitted with ODRPACK²⁷ to the data for the thermal conductivity of propene. The value of $\bar{q}_D^{-1} = 4.3 \times 10^{-10}$ m was found. The crossover model requires the

system-dependent amplitudes Γ and ξ_0 . Following the procedure used for propene, we used the method presented in Perkins *et al.*²⁸ to compute $\Gamma = 0.057$, $\xi_0 = 0.198 \times 10^{-9}$ m. The viscosity required for Eq. (6) was estimated by an extended corresponding-states method of Huber *et al.*⁶¹ The reference temperature T_{ref} , far above the critical temperature where the critical enhancement is negligible, was calculated by $T_{\text{ref}} = (3/2) T_c$,⁵⁶ which for propene is 546.32 K. The coefficients $B_{1,i}$ and $B_{2,i}$ of Eq. (5) obtained are shown in Table 7.

Table 8 summarizes comparisons of the primary data with the correlation. We have defined the percentage deviation as $\text{PCTDEV} = 100 * (\lambda_{\text{exp}} - \lambda_{\text{fit}}) / \lambda_{\text{fit}}$, where λ_{exp} is the experimental value of the thermal conductivity and λ_{fit} is the value calculated from the correlation. Thus, the average absolute percentage deviation (AAD) is found with the expression $\text{AAD} = (\sum |\text{PCTDEV}|) / n$, where the summation is over all n points, and the bias percent is found with the expression $\text{BIAS} = (\sum \text{PCTDEV}) / n$. We estimate the uncertainty (at the 95% confidence level) for the thermal conductivity from 180 K to 625 K at pressures up to 50 MPa to be 5% for the liquid and supercritical phases. Uncertainties in the critical region are much larger, since the thermal conductivity approaches infinity at the critical point and is very sensitive to small changes in density.

Figure 15 shows the percentage deviations of all primary thermal-conductivity data from the values calculated by Eqs. (1), (5)–(9), and (18), as a function of density. Figures 16 and 17 show the same deviations but as a function of temperature and pressure, respectively. Finally, Figs. 18 and 19 show plots of the thermal conductivity of propene as a function of the temperature for different pressures, and as a function of the density for different temperatures.

3.2.3. Empirical critical enhancement—For applications at state points that are relatively distant from the critical point (at least 10–15 K from the critical temperature), the critical enhancement is adequately represented by the following empirical expression:

$$\Delta\lambda_c(\rho, T) = \frac{C_1}{C_2 + |\Delta T_c|} \exp \left[-(C_3 \Delta\rho_c)^2 \right], \quad (19)$$

where $\Delta T_c = (T/T_c) - 1$ and $\Delta\rho_c = (\rho/\rho_c) - 1$. This equation does not require accurate information on the compressibility, specific heat, and viscosity of propene in the critical region, as does the theory of Olchowy and Sengers.^{15, 26, 28} The coefficients of Eqs. (8) and (9) were fixed, while the coefficients of Eq. (19) were fitted to the primary data. The values obtained were $C_1 = 0.20 \text{ mW m}^{-1} \text{ K}^{-1}$, $C_2 = 0.30$, and $C_3 = 0.20$.

3.2.4. Recommended Values—In Table 9, recommended values for the thermal conductivity of propene are shown. For checking computer implementations of the correlation, a point is provided for testing code with critical enhancement at 350.0 K, and 385.0 kg m⁻³ (3.6893 MPa), where the liquid thermal conductivity is 81.47 mW m⁻¹ K⁻¹; the dilute-gas thermal conductivity, $\lambda_o(350 \text{ K}) = 23.07 \text{ mW m}^{-1} \text{ K}^{-1}$, the residual term $\Delta\lambda(385.0 \text{ kg m}^{-3}, 350 \text{ K}) = 53.88 \text{ mW m}^{-1} \text{ K}^{-1}$, and the critical enhancement term, $\Delta\lambda_c(385.0 \text{ kg m}^{-3}, 350 \text{ K}) = 4.52 \text{ mW m}^{-1} \text{ K}^{-1}$. The viscosity used in the calculation of the

enhancement for this state point is 53.841 $\mu\text{Pa s}$, obtained from the corresponding states model of Ref. 61.

4. Conclusion

New, wide-ranging reference equations for the thermal conductivity of ethene and propene were presented. The equations are based in part upon a body of experimental data that has been critically assessed for internal consistency and for agreement with theory whenever possible. In the case of the dilute-gas thermal conductivity, a theoretically based correlation was adopted in order to guide extrapolation behavior. In the critical region, the enhancement of the thermal conductivity is well represented by a theoretically based model.²⁸ The remaining contribution to the thermal conductivity was obtained by fitting critically-assessed data to an empirical equation that is a function of temperature and density.

For ethane, the correlation is valid from 110 K to 680 K and up to 200 MPa, and we estimate the uncertainty (at the 95% confidence level) for the thermal conductivity from 110 K to 520 K at pressures up to 200 MPa to be 5% for the compressed liquid and supercritical phases. For the low-pressure gas phase (to 0.1 MPa) over the temperature range 270 K to 680 K, the estimated uncertainty is 4%. The equation of state of Smukala *et al.*¹¹ is valid from the triple point (103.986 K) to 450 K at pressures up to 300 MPa. The correlation behaves in a physically reasonable manner over this entire range and we feel it can be used over the entire range, although the uncertainty will be large in high-pressure (200 - 300 MPa) regions where there were no experimental data. It is difficult to assign an uncertainty where there are no data; we estimate uncertainty of 10%. In the case of propene, the correlation is valid from 180 K to 625 K and up to 50 MPa, and we estimate the uncertainty (at the 95% confidence level) for the thermal conductivity from 180 K to 625 K at pressures up to 50 MPa to be 5% for the gas, liquid and supercritical phases. The equation of state for propene¹² is valid up to 1000 MPa; this is well above the upper limits of the data used to develop the correlation (50 MPa). Although the correlation behaves in a physically reasonable manner, we do not recommend the use of the correlation above 100 MPa. In addition, the propene equation of state is valid to the triple point, 87.953 K, which is considerably lower than the range of experimental data. In the regions of extrapolation from 50–100 MPa, and for temperatures below 180 K the uncertainty will be larger, estimated to be 10%. For both correlations, uncertainties in the critical region are also much larger, since the thermal conductivity approaches infinity at the critical point and is very sensitive to small changes in density.

References

1. Assael MJ, Assael JAM, Huber ML, Perkins RA, Takata Y. J Phys Chem Ref Data. 2011; 40:033101.
2. Huber ML, Perkins RA, Friend DG, Sengers JV, Assael MJ, Metaxa IN, Miyagawa K, Hellmann R, Vogel E. J Phys Chem Ref Data. 2012; 41:033102.
3. Assael MJ, Koini IA, Antoniadis KD, Huber ML, Abdulagatov IM, Perkins RA. J Phys Chem Ref Data. 2012; 41:023104.
4. Assael MJ, Mylona SK, Huber ML, Perkins RA. J Phys Chem Ref Data. 2012; 41:023101.
5. Assael MJ, Mihailidou EK, Huber ML, Perkins RA. J Phys Chem Ref Data. 2012; 41:043102.
6. Assael MJ, Mylona SK, Huber ML, Perkins RA. J Phys Chem Ref Data. 2013; 42:013106.

7. Assael MJ, Bogdanou I, Mylona SK, Huber ML, Perkins RA, Vesovic V. *J Phys Chem Ref Data*. 2013; 42:023101.
8. Sykioti EA, Assael MJ, Huber MH, Perkins RA. *J Phys Chem Ref Data*. 2013; 42:043101.
9. Assael MJ, Sykioti EA, Huber ML, Perkins RA. *J Phys Chem Ref Data*. 2013; 42:023102.
10. Mylona SK, Antoniadis KD, Assael MJ, Huber ML, Perkins RA. *J Phys Chem Ref Data*. 2014; 43:043104.
11. Smukala J, Span R, Wagner W. *J Phys Chem Ref Data*. 2000; 29:1053.
12. Lemmon EW, McLinden MO, Overhoff U, Wagner W. A Reference Equation of State for Propene for Temperatures from the Melting Line to 575 K and Pressures up to 1000 MPa. *J Phys Chem Ref Data*. 2016 to be submitted.
13. Holland PM, Eaton BE, Hanley HJM. *J Phys Chem Ref Data*. 1983; 12:917.
14. Millat J, Ross M, Wakeham WA, Zalaf M. *Int J Thermophys*. 1988; 9:481.
15. Olchoway GA, Sengers JV. *Phys Rev Lett*. 1988; 61:15. [PubMed: 10038682]
16. Olchoway GA, Sengers JV. *Int J Thermophys*. 1989; 10:417.
17. Assael MJ, Ramires MLV, Nieto de Castro CA, Wakeham WA. *J Phys Chem Ref Data*. 1990; 19:113.
18. Hellmann R, Bich E, Vogel E, Vesovic V. *J Chem Eng Data*. 2012; 57:1312.
19. McCourt, FRW.; Beenakker, JJM.; Köhler, WE.; Kučšer, I. *Nonequilibrium Phenomena in Polyatomic Gases*. Clarendon Press; Oxford: 1990.
20. Thijsse BJ, Thoof GW, Coombe DA, Knaap HFP, Beenakker JJM. *Physica A*. 1979; 98:307.
21. Millat J, Vesovic V, Wakeham WA. *Physica A*. 1988; 148:153.
22. Bock S, Bich E, Vogel E, Dickinson AS, Vesovic V. *J Chem Phys*. 2004; 120:7987. [PubMed: 15267716]
23. Hellmann R, Bich E, Vogel E, Dickinson AS, Vesovic V. *J Chem Phys*. 2009; 130:124309. [PubMed: 19334832]
24. Hellmann R, Bich E, Vogel E, Vesovic V. *Phys Chem Chem Phys*. 2011; 13:13749. [PubMed: 21720616]
25. Mostert R, van den Berg HR, van der Gulik PS, Sengers JV. *J Chem Phys*. 1990; 92:5454.
26. Perkins RA, Roder HM, Friend DG, Nieto de Castro CA. *Physica A*. 1991; 173:332.
27. Boggs, PT.; Byrd, RH.; Rogers, JE.; Schnabel, RB. *ODRPACK, Software for Orthogonal Distance Regression, NISTIR 4834, v2.013*. National Institute of Standards and Technology; Gaithersburg, MD: 1992.
28. Perkins RA, Sengers JV, Abdulagatov IM, Huber ML. *Int J Thermophys*. 2013; 34:191.
29. Zheng XY, Yamamoto S, Yoshida H, Masuoka H, Yorizane M. *J Chem Eng Jpn*. 1984; 17:237.
30. Yorizane M, Yoshimura S, Masuoka H, Yoshida H. *Ind Eng Chem Fundam*. 1983; 22:454.
31. Prasad RC, Venart JES. *Proc of 8th Symp on Thermophys Prop*. 1981; 1:263.
32. Vargaftik NB, Vanicheva NA. *J Eng Phys (Engl Transl)*. 1974; 27:978.
33. Tarzimanov AA, Lozovoi VS. *Teplofiz Svoistva Gazov, Mater Vses Teplofiz Konf Svoistvam Veshchestv Vys Temp*. 1973; 4:18.
34. Tarzimanov A, Arslanov VA. *Tepl I Massoperenos*. 1972; 7:81.
35. Golubev IF, Shpagina IB, Mamonov YV. *Tr Nauchno-Issled Proektn Inst Azotn Prom Prod Org Sin*. 1971; 8:81.
36. Senftleben H. *Z Angew Phys*. 1964; 17:86.
37. Lambert JD, Cotton KJ, Pailthorpe MW, Robinson AM, Scrivins J, Vale WRF, Young RM. *Proc R Soc London A*. 1955; 231:280.
38. Senftleben H. *Z Angew Phys*. 1953; 5:33.
39. Lenoir J, Comings EW. *Chem Eng Progr*. 1951; 47:223.
40. Senftleben H, Gladisch H, Recklinghausen K. *Z Phys*. 1949; 125:653.
41. Borovick Y. *Zh Tekh Fiz*. 1947; 17:328.
42. Borovick Y, Matveyev A, Panina Y. *Zh Tekh Fiz*. 1940; 10:988.
43. Eucken A. *Phys Z*. 1913; 14:324.

44. Aggarwal MC, Springer GS. *J Chem Phys.* 1979; 70:2948.
45. Gray P, Parkinson C. *J Chem Soc Faraday Trans 1.* 1974; 70:560.
46. Kolomiets AY. *Heat Transfer - Sov Res.* 1974; 6:42.
47. Neduzhii IA, Kolomiets AY, Veshchestv TS. *Teplfiz Svoistva Veshchestv.* 1969; 84
48. Naziev YM, Abasov AA. *Izv Vyssh Uchebn Zaved, Neft Gaz.* 1968; 11:63.
49. Cheung H, Bromley LA, Wilke CR. *AIChE J.* 1962; 8:221.
50. Chaikin AM, Markevich AM. *Zh Fiz Khim.* 1958; 32:116.
51. Keyes FG. *Trans ASME.* 1954; 76:809.
52. Eucken A. *Forsch Geb Ingenieurwes.* 1940; 11:6.
53. Preston-Thomas H. *Metrologia.* 1990; 27:3.
54. Wakeham, WA.; Nagashima, A.; Sengers, JV., editors. *Experimental Thermodynamics Volume III. Measurement of the Transport Properties of Fluids.* Blackwell Scientific Publications; Oxford, U.K: 1991.
55. Assael, MJ.; Goodwin, ARH.; Vesovic, V.; Wakeham, WA., editors. *Experimental Thermodynamics Volume IX. Advances in Transport Properties of Fluids.* The Royal Society of Chemistry; Cambridge, U.K: 2015.
56. Vesovic V, Wakeham WA, Olchoway GA, Sengers JV. *J Phys Chem Ref Data.* 1990; 19:763.
57. Yata J, Hori M, Isono Y, Ueda Y. *Thermal Conductivity 25: Thermal Expansion 13: joint conferences.* 1999; 325
58. Swift GW, Migliori A. *J Chem Eng Data.* 1984; 29:56.
59. Parkinson C, Mukhopadhyay P, Gray P. *J Chem Soc, Faraday Trans 1.* 1972; 68:1077.
60. Naziev, YM. *Proc. Fifth Symp. Thermophysical Properties; Boston, Mass.* 1970. p. 8-14.
61. Huber ML, Laesecke A, Perkins RA. *Ind Eng Chem Res.* 2003; 42:3163.

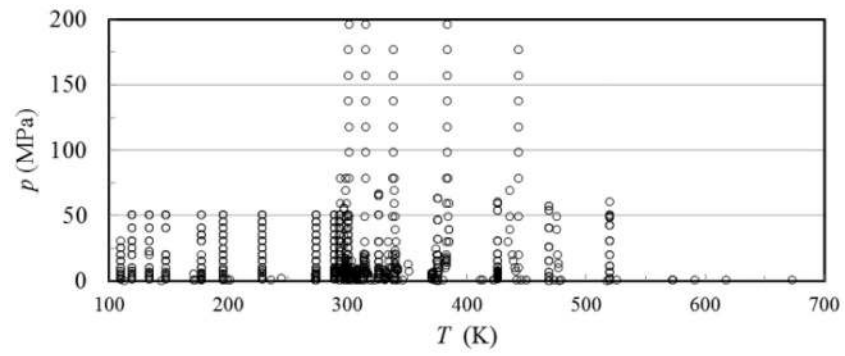


FIGURE 1.
Temperature–pressure range of the primary experimental thermal conductivity data for ethene.

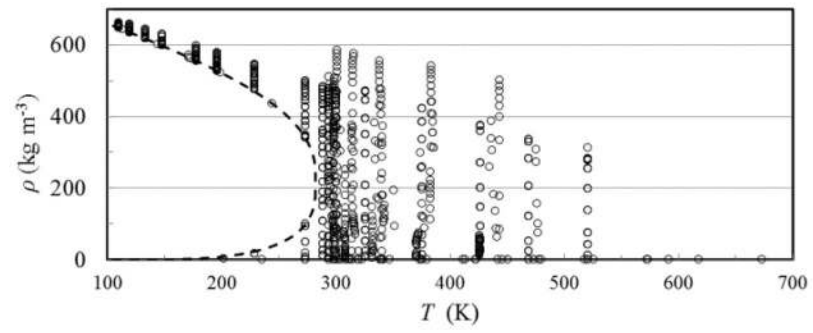


FIGURE 2. Temperature–density range of the primary experimental thermal conductivity data for ethene. (– –) saturation curve.

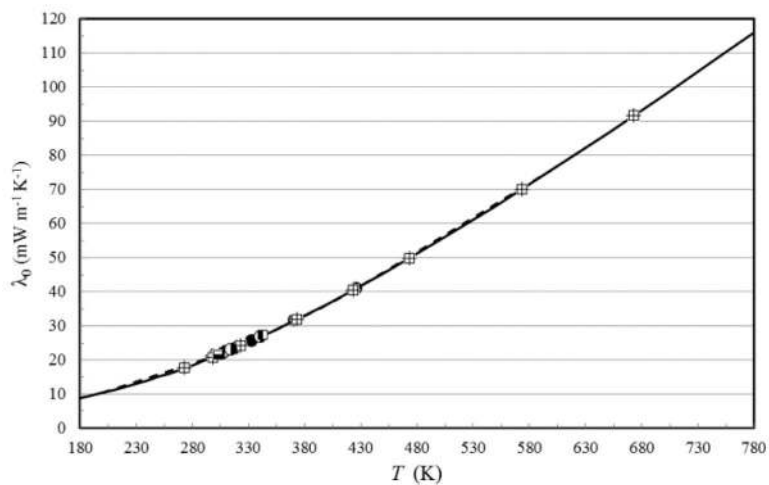


FIGURE 3.

Primary Dilute-gas thermal-conductivity of ethene as a function of temperature. Millat *et al.*¹⁴ (●), Zheng *et al.*²⁹ (◆), Yorizane *et al.*³⁰ (◊), Senftleben³⁶ (⊕), Senftleben³⁸ (■), Lenoir and Comings³⁹ (●), Senftleben *et al.*⁴⁰, Eq. (13) (—), and correlation of Holland *et al.*¹³ (- -).

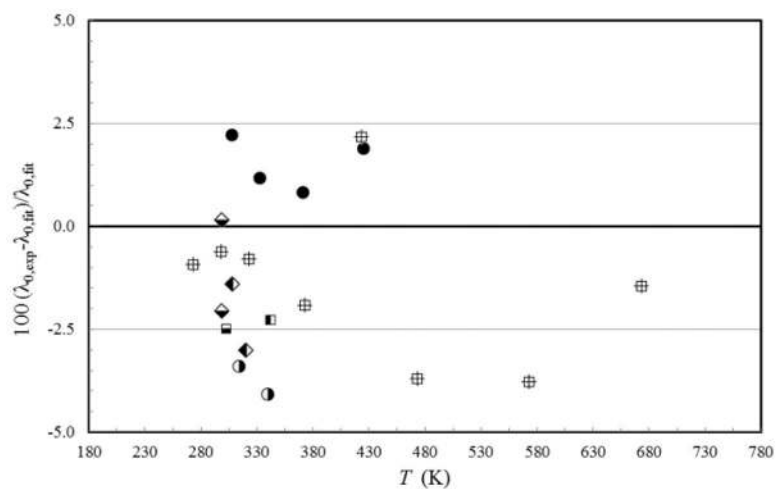


FIGURE 4. Percentage deviations of the primary dilute-gas thermal-conductivity measurements of ethene from the scheme of Eqs. (10)–(12) as a function of temperature. Millat *et al.*¹⁴ (●), Zheng *et al.*²⁹ (◆), Yorizane *et al.*³⁰ (◇), Senftleben³⁶ (⊕), Senftleben³⁸ (■), Lenoir and Comings³⁹ (●), Senftleben *et al.*⁴⁰ (■), Eq. (13) (—).

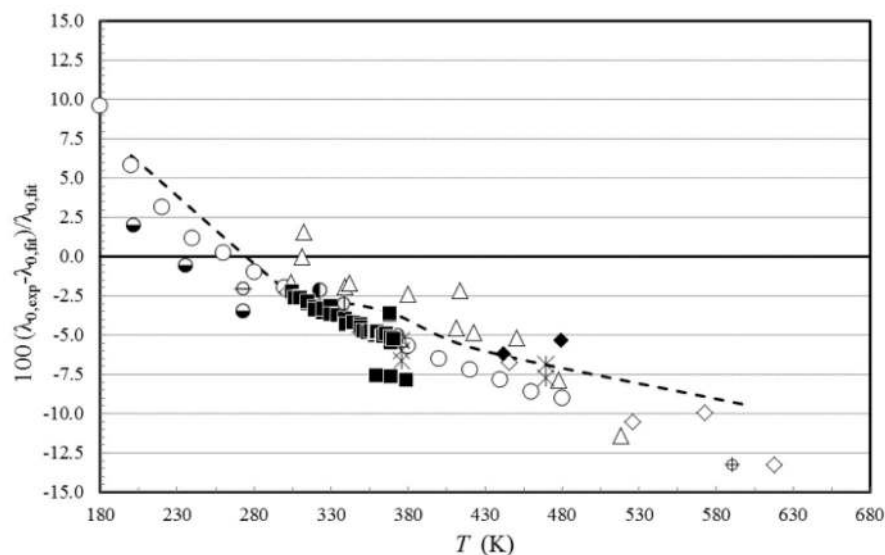


FIGURE 5. Percentage deviations of the secondary dilute-gas thermal conductivity measurements of ethene from the scheme of Eqs. (10)–(12) as a function of temperature. Gray and Parkinson⁴⁵ (●), Kolomiets⁴⁶ (○), Vargaftik and Vanicheva³² (△), Tarzimanov and Lozovoi³³ (◆), Tarzimanov and Arslanov³⁴ (◇), Golubev *et al.*³⁵ (*), Neduzhii *et al.*⁴⁷ (■), Cheung *et al.*⁴⁹ (⊕), Chaikin and Markevich⁵⁰ (▲), Lambert *et al.*³⁷ (Φ), Eucken⁵² (⊖), Eucken⁴³ (⊙), correlation of Holland *et al.*¹³ (---), Eq. (13) (—).

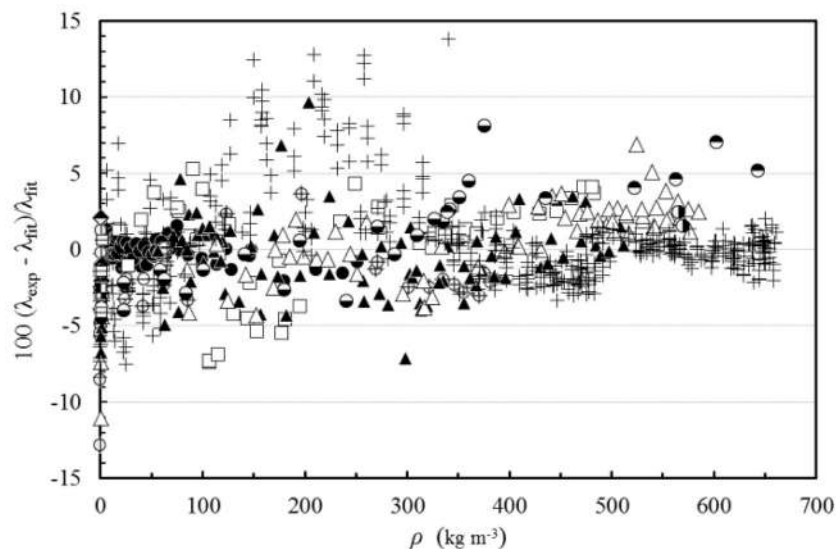


FIGURE 6. Percentage deviations of primary experimental data of ethene from the values calculated by the present model, Eqs. (1), (5)–(9), and (13), as a function of density. Millat *et al.*¹⁴ (●), Zheng *et al.*²⁹ (⊕), Yorzane *et al.*³⁰ (⊖), Prasad and Venart³¹ (□), Vargaftik and Vanicheva³² (⊕), Tarzimanov and Lozovoi³³ (▲), Tarzimanov and Arslanov³⁴ (△), Golubev *et al.*³⁵ (+), Senftleben³⁶ (⊕), Lambert *et al.*³⁷ (■), Senftleben³⁸ (■), Lenoir and Comings³⁹ (⊖), Senftleben *et al.*⁴⁰ (■), Borovick⁴¹ (⊖), Borovick *et al.*⁴² (⊖), Eucken⁴³ (⊕).

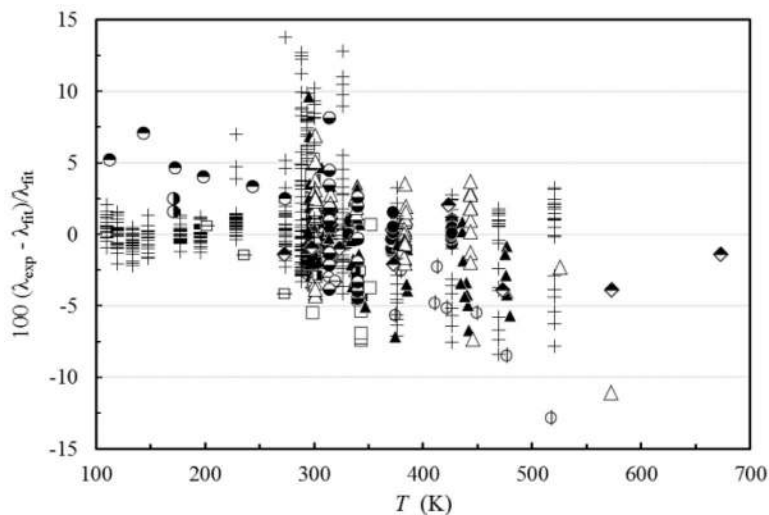


FIGURE 7.

Percentage deviations of primary experimental data of ethene from the values calculated by the present model, Eqs. (1), (5)–(9), and (13), as a function of temperature. Millat *et al.*¹⁴ (●), Zheng *et al.*²⁹ (⊕), Yorizane *et al.*³⁰ (⊖), Prasad and Venart³¹ (□), Vargaftik and Vanicheva³² (⊕), Tarzimanov and Lozovoi³³ (▲), Tarzimanov and Arslanov³⁴ (△), Golubev *et al.*³⁵ (+), Senftleben³⁶ (◆), Lambert *et al.*³⁷ (▣), Senftleben³⁸ (▢), Lenoir and Comings³⁹ (⊙), Senftleben *et al.*⁴⁰ (▣), Borovick⁴¹ (⊙), Borovick *et al.*⁴² (⊙), Eucken⁴³ (⊕).

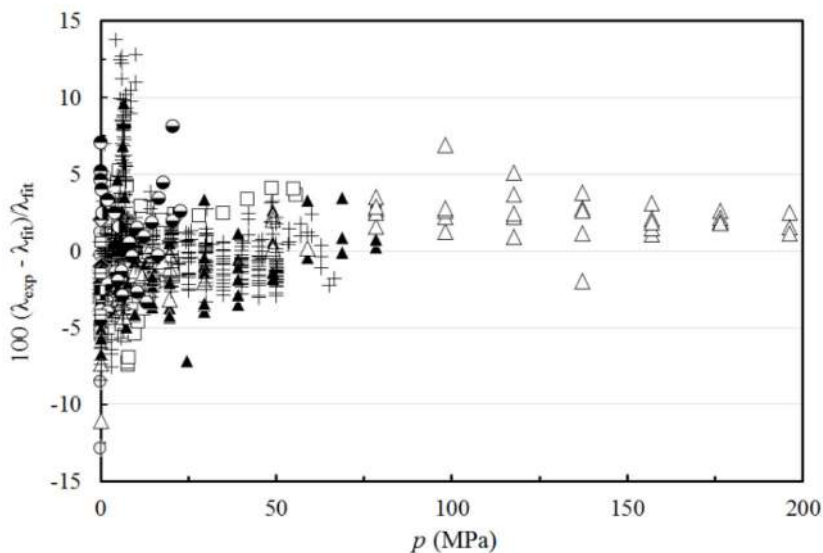


FIGURE 8.

Percentage deviations of primary experimental data of ethene from the values calculated by the present model, Eqs. (1), (5)–(9), and (13), as a function of pressure. Millat *et al.*¹⁴ (●), Zheng *et al.*²⁹ (⊕), Yorizane *et al.*³⁰ (⊖), Prasad and Venart³¹ (□), Vargaftik and Vanicheva³² (⊕), Tarzimanov and Lozovoi³³ (▲), Tarzimanov and Arslanov³⁴ (△), Golubev *et al.*³⁵ (+), Senftleben³⁶ (⊕), Lambert *et al.*³⁷ (■), Senftleben³⁸ (■), Lenoir and Comings³⁹ (⊖), Senftleben *et al.*⁴⁰ (■), Borovick⁴¹ (○), Borovick *et al.*⁴² (●), Eucken⁴³ (⊕).

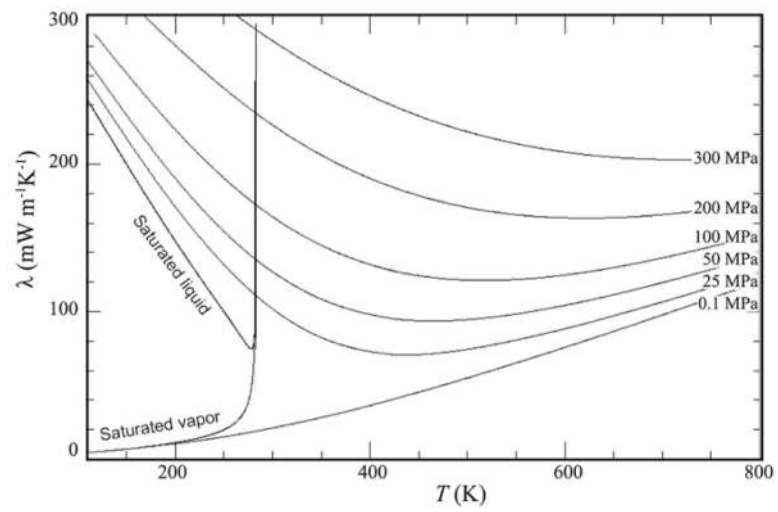


FIGURE 9.
Thermal conductivity of ethene as a function of temperature for different pressures.

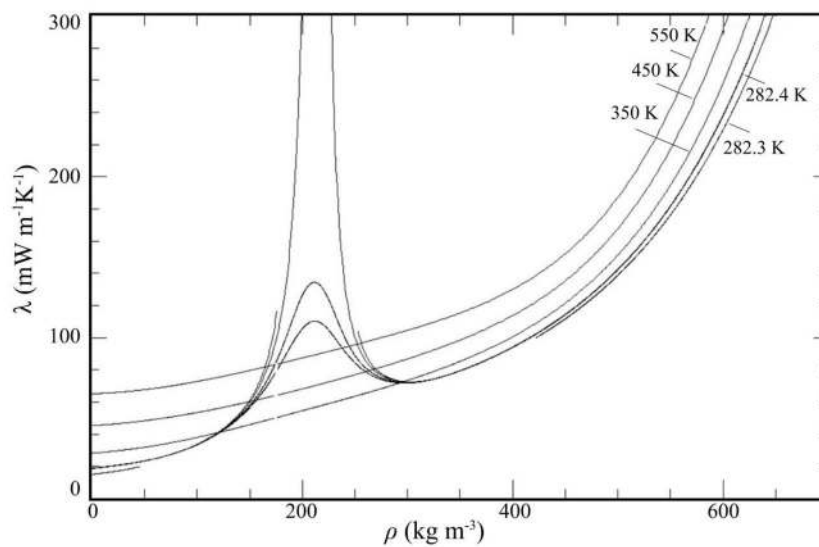


FIGURE 10.
Thermal conductivity of ethene as a function of density for different temperatures.

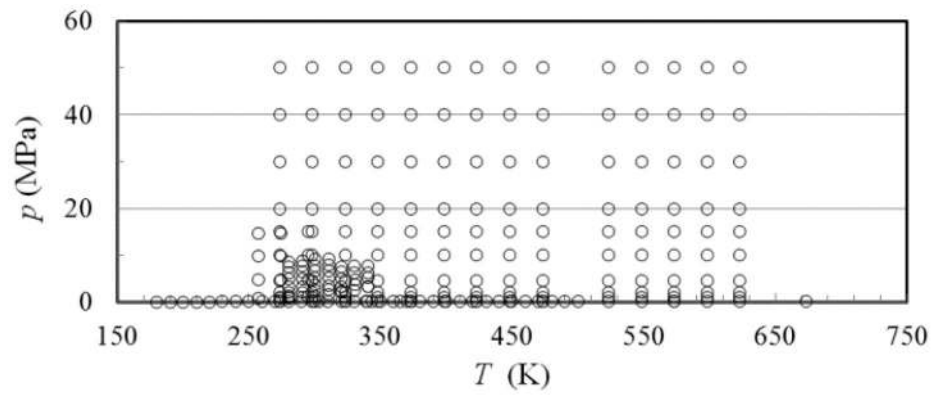


FIGURE 11.
Temperature–pressure range of the primary experimental thermal conductivity data for propene.

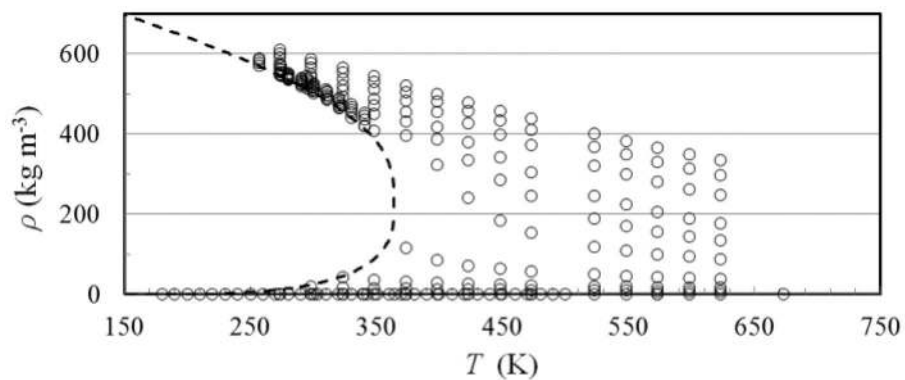
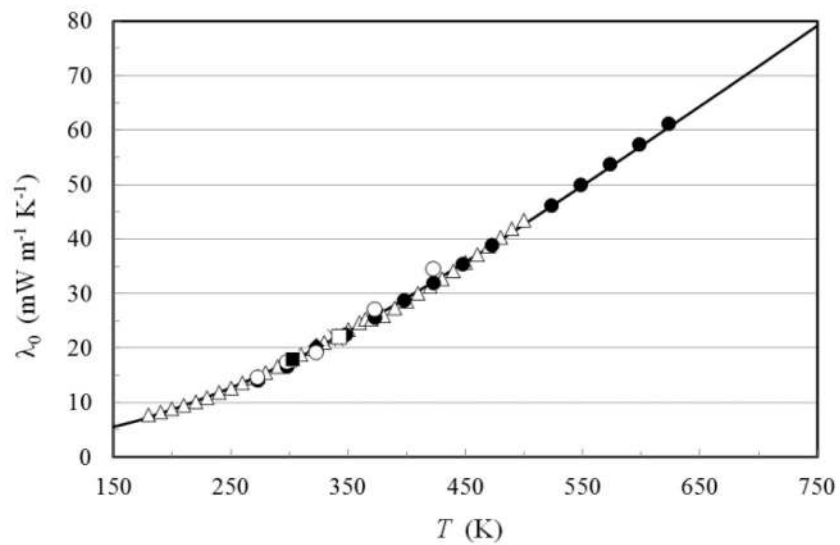


FIGURE 12. Temperature–density range of the primary experimental thermal conductivity data for propene. (– –) saturation curve.

**FIGURE 13.**

Primary dilute-gas thermal-conductivity of propene as a function of temperature.

Kolomiets⁴⁶ (Δ), Parkinson *et al.*⁵⁹ (\blacktriangle), Naziev⁶⁰ (\bullet), Senftleben³⁶ (\circ), Lambert *et al.*³⁷ ($*$), Senftleben³⁸ (\blacksquare), Senftleben *et al.*⁴⁰ (\square), and Eq. (18) ($_$).

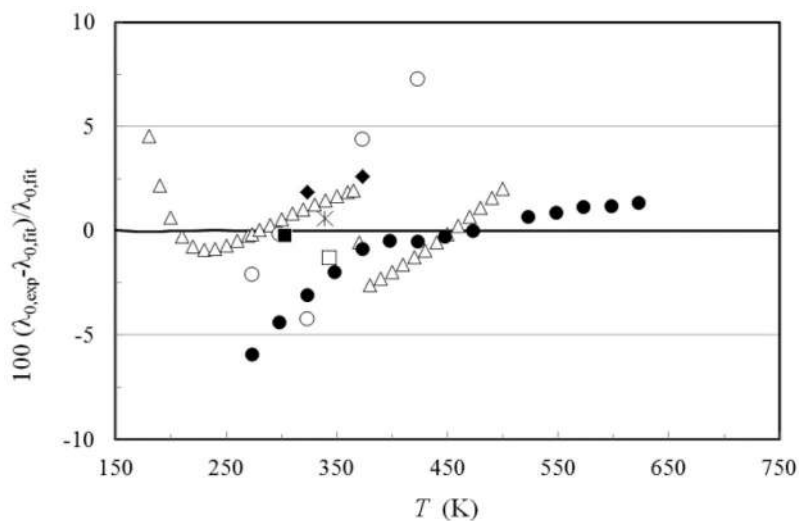


FIGURE 14.

Percentage deviations of the primary dilute-gas thermal-conductivity measurements of propene from the scheme of Eqs. (15)–(17) as a function of temperature. Kolomiets⁴⁶ (Δ), Parkinson *et al.*⁵⁹ (\blacktriangle), Naziev⁶⁰ (\bullet), Senftleben³⁶ (\circ), Lambert *et al.*³⁷ ($*$), Senftleben³⁸ (\blacksquare), Senftleben *et al.*⁴⁰ (\square), and Eq. (18) ($_$).

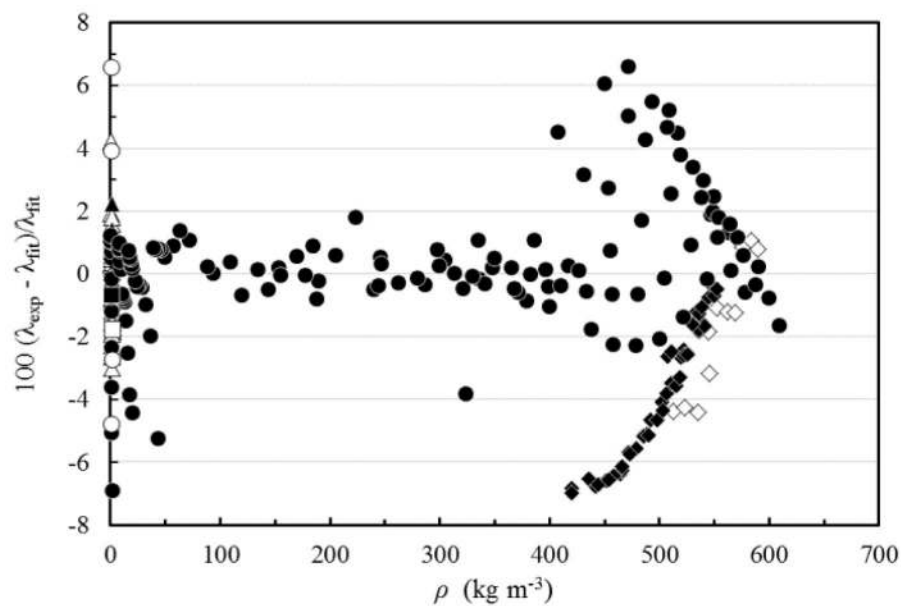


FIGURE 15.

Percentage deviations of primary experimental data of propene from the values calculated by the present model, Eqs. (1), (5)–(9), and (18), as a function of density. Yata *et al.*⁵⁷ (\diamond), Swift and Migliori⁵⁸ (\blacklozenge), Kolomiets⁴⁶ (\triangle), Parkinson *et al.*⁵⁹ (\blacktriangle), Naziev⁶⁰ (\bullet), Senftleben³⁶ (\circ), Lambert *et al.*³⁷ (\ast), Senftleben³⁸ (\blacksquare), Senftleben *et al.*⁴⁰ (\square).

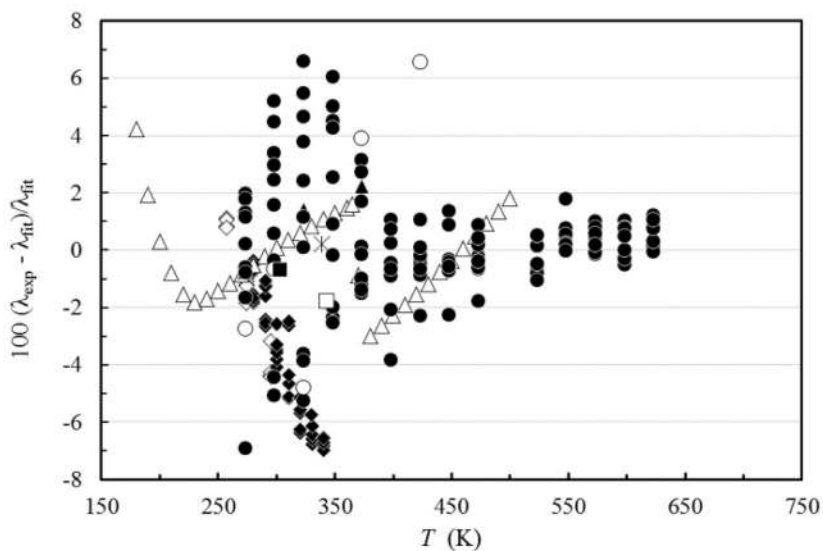


FIGURE 16.

Percentage deviations of primary experimental data of propene from the values calculated by the present model, Eqs. (1), (5)–(9), and (18), as a function of temperature. Yata *et al.*⁵⁷ (\diamond), Swift and Migliori⁵⁸ (\blacklozenge), Kolomiets⁴⁶ (\triangle), Parkinson *et al.*⁵⁹ (\blacktriangle), Naziev⁶⁰ (\bullet), Senftleben³⁶ (\circ), Lambert *et al.*³⁷ ($*$), Senftleben³⁸ (\blacksquare), Senftleben *et al.*⁴⁰ (\square).

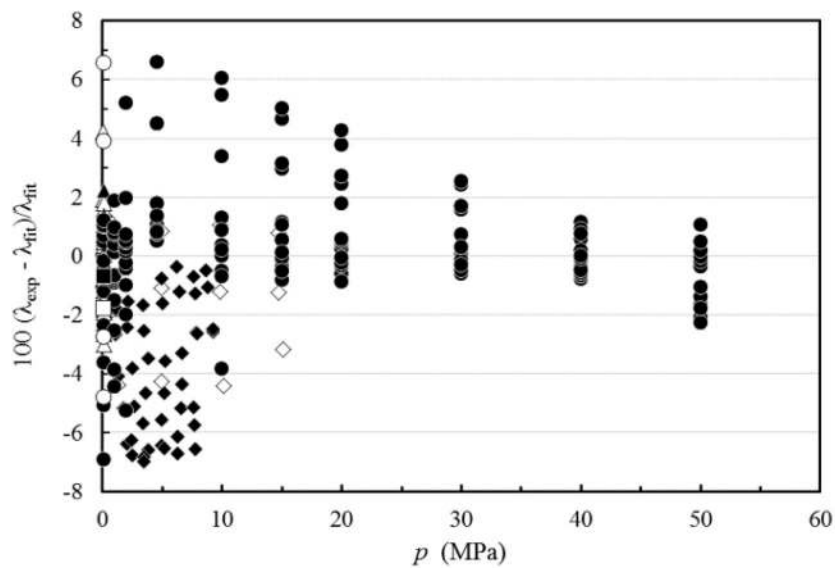


FIGURE 17.

Percentage deviations of primary experimental data of propene from the values calculated by the present model, Eqs. (1), (5)–(9), and (18), as a function of pressure. Yata *et al.*⁵⁷ (\diamond), Swift and Migliori⁵⁸ (\blacklozenge), Kolomiets⁴⁶ (\triangle), Parkinson *et al.*⁵⁹ (\blacktriangle), Naziev⁶⁰ (\bullet), Senftleben³⁶ (\circ), Lambert *et al.*³⁷ (\ast), Senftleben³⁸ (\blacksquare), Senftleben *et al.*⁴⁰ (\square).

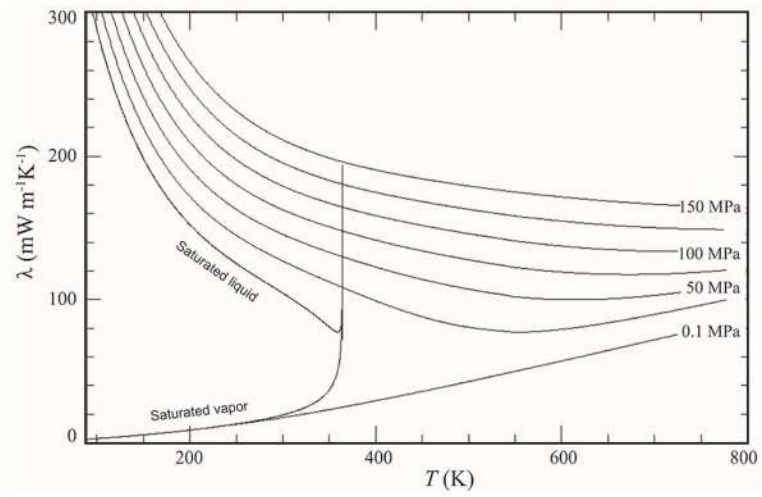


FIGURE 18.
Thermal conductivity of propene as a function of temperature for different pressures.

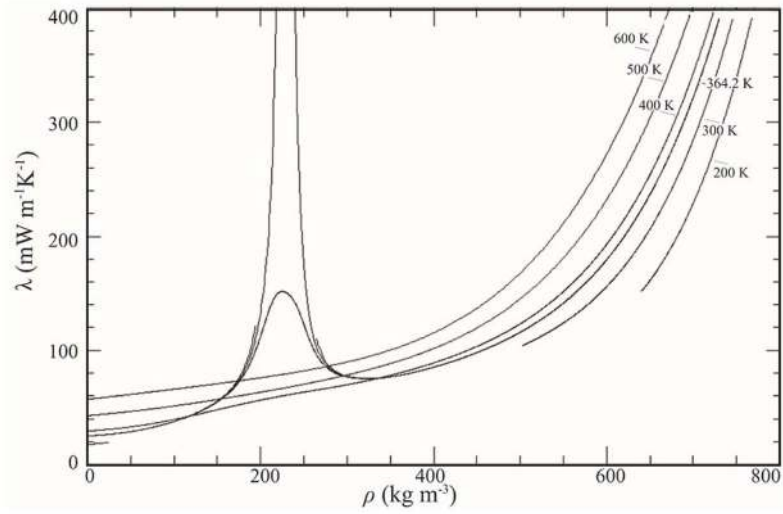


FIGURE 19. Thermal conductivity of propene as a function of density for different temperatures.

TABLE 1

Thermal-conductivity measurements of ethene

1 st author	Year Publ.	Technique employed ^a	Purity (%)	Uncertainty (%)	No. of data	Temperature range (K)	Pressure range (MPa)
Primary Data							
Millat ¹⁴	1988	THW	99.92	0.3–2	69	308–426	0.4–8.8
Zheng ²⁹	1984	CC	99.5	3	20	299	0.1–17
Yorizane ³⁰	1983	CC	99.5	3	21	293–320	0.1–4.3
Prasad ³¹	1981	THW	99.95	1.5	41	297–352	1.4–56
Vargafik ³²	1974	HF	na	1–2	12	304–518	0.01–0.4
Tarzmanov ³³	1973	HW	99.98	1.5–3	89	294–479	0.1–79
Tarzmanov ³⁴	1972	HW	99.99	1.5–3	68	301–618	0.1–196
Golubev ³⁵	1971	HW	99.9	1.5–3	537	293–521	0.1–67
Senfleben ³⁶	1964	CC	na	1–2	8	273–673	0.1
Lambert ³⁷	1955	HW	na	na	1	339	0.1
Senfleben ³⁸	1953	CC	na	1–4	1	273	0.1
Lenoir ³⁹	1951	CC	na	1.5	21	314–241	0.1–23
Senfleben ⁴⁰	1949	CC	na	1	1	343	0.1
Borovick ⁴¹	1947	PP	na	na	2	172	0.5–6
Borovick ⁴²	1940	HW	99.8	2.6	6	112–274	0.0005–4.1
Eucken ⁴³	1913	HW	na	na	3	202–273	0.1
Secondary Data							
Aggarwal ⁴⁴	1979	HF	99.5	1	48	400–750	0.1–2.7
Gray ⁴⁵	1974	THW	99	3	2	323–373	0.1
Kolomitets ⁴⁶	1974	HW	99.99	1–2.5	176	180–480	0.1–50
Neduzhii ⁴⁷	1969	HW	99.9	na	41	304–379	0.1
Naziev ⁴⁸	1968	CC	99.9	na	14	273–533	0.1
Cheung ⁴⁹	1962	CC	na	2.1	1	591	0.1
Chaikin ⁵⁰	1958	CC	na	10	6	293–523	0.1
Keyes ⁵¹	1954	CC	na	na	6	342–425	0–1.6
Eucken ⁵²	1940	HW	na	na	1	273	0.1

^aCC, coaxial cylinder; HW, hot wire; HF, hot filament; na, not available; PP, parallel plate; THW, transient hot wire.

NIST Author Manuscript

NIST Author Manuscript

NIST Author Manuscript

TABLE 2

Coefficients of Eq. (5) for the residual thermal conductivity of ethene.

i	$B_{1,i} (\text{mW m}^{-1} \text{K}^{-1})$	$B_{2,i} (\text{mW m}^{-1} \text{K}^{-1})$
1	$0.261\,453 \times 10^{+2}$	$-0.113\,225 \times 10^{+2}$
2	$-0.218\,619 \times 10^{+2}$	$0.269\,282 \times 10^{+2}$
3	$0.362\,068 \times 10^{+2}$	$-0.223\,164 \times 10^{+2}$
4	$-0.136\,642 \times 10^{+2}$	$0.390\,241 \times 10^{+1}$
5	$0.184\,752 \times 10^{+1}$	$0.668\,286 \times 10^{+0}$

TABLE 3

Evaluation of the ethene thermal-conductivity correlation for the primary data.

1st Author	Year Publ.	AAD (%)	BIAS (%)
Millat ¹⁴	1988	0.52	-0.07
Zheng ²⁹	1984	2.30	-1.71
Yorizane ³⁰	1983	2.03	-2.03
Prasad ³¹	1981	2.91	0.32
Vargaftik ³²	1974	4.23	-4.04
Tarzimanov ³³	1973	2.11	-0.52
Tarzimanov ³⁴	1972	2.49	0.17
Golubev ³⁵	1971	2.42	0.83
Senftleben ³⁶	1964	2.12	-1.61
Lambert ³⁷	1955	3.37	-3.37
Senftleben ³⁸	1953	2.92	-2.92
Lenoir ³⁹	1951	2.58	-0.17
Senftleben ⁴⁰	1949	2.55	-2.55
Borovick ⁴¹	1947	2.00	2.00
Borovick ⁴²	1940	4.43	4.43
Eucken ⁴³	1913	2.06	-1.66
Entire data set		2.44	0.05

NIST Author Manuscript

NIST Author Manuscript

NIST Author Manuscript

TABLE 4

Evaluation of the ethene thermal–conductivity correlation for the secondary data.

1st Author	Year Publ.	AAD (%)	BIAS (%)
Aggarwal ⁴⁴	1979	16.39	-16.39
Gray ⁴⁵	1974	4.00	-4.00
Kolomiets ⁴⁶	1974	3.82	-2.21
Neduzhii ⁴⁷	1969	4.68	-4.68
Naziev ⁴⁸	1968	9.02	-9.02
Cheung ⁴⁹	1962	15.34	-15.34
Chaikin ⁵⁰	1958	8.33	-7.71
Keyes ⁵¹	1954	3.70	-3.70
Eucken ⁵²	1940	2.67	-2.67

TABLE 5Recommended values of ethene thermal conductivity ($\text{mW m}^{-1} \text{K}^{-1}$)

Pressure (MPa)	Temperature (K)			
	200	300	400	500
0	10.39	21.01	36.36	55.05
0.1	10.54	21.09	36.40	55.06
50	190.4	126.9	98.08	94.56
100	223.5	164.3	132.0	121.3
150	252.9	196.4	161.7	145.8
200	280.5	226.5	190.3	170.6

NIST Author Manuscript

NIST Author Manuscript

NIST Author Manuscript

TABLE 6

Thermal-conductivity measurements of propene

1 st author	Year Publ.	Technique employed ^a	Purity (%)	Uncertainty (%)	No. of data	Temperature range (K)	Pressure range (MPa)
Primary Data Yata ⁵⁷	1999	THW	99.5	1	12	257–295	0.8–15.0
Swift ⁵⁸	1984	THW	99.0	3	46	280–340	0.8–9.2
Kolomiets ⁴⁶	1974	HW	99.9	na	35	180–500	0.1
Parkinson ⁵⁹	1972	THW	99.0	2	2	293	0.1
Naziev ⁶⁰	1970	CC	99.9	1.4	140	273–623	0.1–50
Senfleben ³⁶	1964	HW	na	na	8	273–423 ^b	0.1
Lambert ³⁷	1955	HW	na	na	1	339	0.1
Senfleben ³⁸	1953	HW	na	1–4	1	293	0.1
Senfleben ⁴⁰	1949	HW	na	1	1	343	0.1

^aCC, coaxial cylinder; HW, hot wire; na, not available; THW, transient hot wire.^bThe last three temperatures over 423 K were not considered.

TABLE 7

Coefficients of Eq. (5) for the residual thermal conductivity of propene.

i	$B_{1,i}$ (mW m ⁻¹ K ⁻¹)	$B_{2,i}$ (mW m ⁻¹ K ⁻¹)
1	0.271 511×10 ⁺¹	0.994 697×10 ⁺¹
2	-0.363 839×10 ⁺²	0.242 705×10 ⁺²
3	0.106 159×10 ⁺³	-0.659 429×10 ⁺²
4	-0.616 755×10 ⁺²	0.379 916×10 ⁺²
5	0.105 424×10 ⁺²	-0.569 120×10 ⁺¹

TABLE 8

Evaluation of the propene thermal-conductivity correlation for the primary data.

1st Author	Year Publ.	AAD (%)	BIAS (%)
Yata	1999	2.12	-1.49
Swift	1984	3.81	-3.81
Kolomiets	1974	1.25	-0.19
Parkinson	1972	1.82	1.82
Naziev	1970	1.46	0.27
Senftleben	1964	3.73	0.45
Lambert	1955	0.22	0.21
Senftleben	1953	0.68	-0.68
Senftleben	1949	1.79	-1.79
Entire data set		1.95	-0.65

NIST Author Manuscript

NIST Author Manuscript

NIST Author Manuscript

TABLE 9Recommended values of propene thermal conductivity ($\text{mW m}^{-1} \text{K}^{-1}$)

Pressure (MPa)	Temperature (K)			
	200	300	400	500
0	8.75	17.55	29.18	42.64
0.1	152.3	17.64	29.25	42.71
25	171.9	126.8	99.09	80.66
50	191.0	145.5	122.6	107.2